Calculations of Linear and Nonlinear Optical Properties of H−Silsesquioxanes

Wen-Dan Cheng,[†,‡] Kai-Hua Xiang,[†] Ravindra Pandey,*[,†] and Udo C. Pernisz[§]

Department of Physics, Michigan Technological University, Houghton, Michigan 49931, and Dow Corning Corporation, Midland, Michigan 48686

Received: January 4, 2000; In Final Form: April 3, 2000

We report the frequency dependence of linear and nonlinear optical susceptibilities of H−silsesquioxanes of various cage sizes and conformations using the INDO/CI method coupled with the SOS method. The average dynamic refractive index of silsesquioxanes is found to decrease as the cage size increases, and its variation is very small for the different conformations of the same cage size at the same incident wavelength. The calculated second-order susceptibilities show that small cages have a larger magnitude which is comparable to that of crystalline α-quartz. It is suggested here that H−silsesquioxanes of a smaller cage size can be a good candidate materials for nonlinear optical applications having low absorption, wide transparency and adequate susceptibility in ultraviolet or vacuum ultraviolet region of the spectrum.

1. Introduction

H−silsesquioxanes (HSQ) constitute an important class of resinous inorganic polymers.[1−4] The structure of this polymer is based on the siloxane-containing cages that are formed from the building block unit of a trifunctional monomer ($HSiO_{3/2}$), designated as T. The cross-linking of various siloxane-containing cages leads to a wide range in the distribution of molecular masses up to 200 kDa for the polymer. Furthermore, the T_8 (i.e., $H_8Si_8O_{12}$) cage has shown to be a suitable starting molecule for the synthesis of higher substituted octanuclear silsesquioxanes.[5]

There has been considerable interest in the fundamental understanding of the structure−property relationship of H−silsesquioxanes due to either their importance in achieving the atomic scale control of the Si/SiO_2 interface[6] or their role in manufacturing of integrated circuits as interlayer dielectric.[7] Recently, we have performed a detailed theoretical study[8] on H−silsesquioxanes (i.e., $(HSiO_{3/2})_n$ with $n = 4$, 6, 8, 10, 12, 14 and 16) where cages of various sizes and conformations were investigated in the framework of density functional theory. One of the revealing feature of this study was the prediction of the presence of a gap state for the large *T* cages suggesting that larger size cages in H−silsesquioxanes could affect the dielectric properties of such materials. We now focus on the linear and nonlinear optical properties of H−silsesquioxanes and report the results of calculations based on a combination of the intermediate neglect of differential overlap (INDO) and the configuration interaction (CI) methods coupled with sum-over-states (SOS) method.[9,10] This approach is demonstrated to be successful in calculating the optical properties of organometallic compounds and inorganic solid compounds.[11,12] To our knowledge, however, experimental or theoretical investigations of optical properties have not yet been reported for this class of polymers.

It is well-known that the polymer-based materials exhibit efficient second-order nonlinear optical properties which can be exploited for optical processing, data storage, and sensors. However, most of the functionalized polymers are either insoluble or have a low solubility which usually requires their more difficult processing them into thin films at high temperatures. Recently, Jiang and Kakkar[13] developed a method by which siloxane linkages can be introduced into the chromophores of a polymer. This leads to higher solubility of the desired polymers, and the second-harmonic generation response from these polymers shows long-term stability at room temperature. We note here that the resinous HSQ polymer, provided it has a sufficiently low molecular weight in the range below ca. 50 kDa, is soluble in many organic solvents; the solution can be spin-cast to give thin films of HSQ which can be cross-linked by low-temperature heat treatment (<400 °C). In an oxidizing ambient, the HSQ film is partially converted into low-density silica. It has been reported[14] that this film has a low dielectric constant (below 3, depending on the heating process) and shows low absorption coefficients with wide spectral range well into the ultraviolet (UV) region, similar to silicon dioxide.

In this work, we have calculated polarizabilities and hyperpolarizabilities of the T_n cages where $n = 4$, 6, 8, 10, 12, 14, and 16 predicting the frequency dependence of refractive indices $n(\omega)$ and the frequency doubling coefficients $\chi^{(2)}(-2\omega;\omega,\omega)$. We find that the increase in the cage size results in lowering of both $n(\omega)$ and $\chi^{(2)}(-2\omega;\omega,\omega)$. Furthermore, $\chi^{(2)}_{xyz}$ of T_4 and $\chi^{(2)}_{zzz}$, $\chi^{(2)}_{zyy}$ of T_8 falls in the range from 0.2 to 20 pm/V, which is found to be sufficient for transparent materials of practical importance for nonlinear frequency conversion.[15] In section 2, a brief description of the computational method and molecular configurations employed in this study is given, and results are presented and discussed in relation to experiments in section 3. A summary of the results of this study is given in section 4.

2. Computational Method

The optical properties of a bulk state (or assembly in our case) can be thought of as being built up from the corresponding properties of individual molecules, and the bulk susceptibility

[†] Michigan Technological University.
[‡] Permanent Address: Fujian Institute of Research on the Structure of Matter, Chinese Academy of Sciences, Fuzhou, Fujian 350002, PRC.
[§] Dow Corning Corporation.

10.1021/jp000016b CCC: $19.00 © 2000 American Chemical Society
Published on Web 06/29/2000

has a relation with the polarizability of a molecule. Therefore, the optical susceptibility of the bulk material can be calculated using the molecular polarizability, local-field correct factor, and molecular number density. In this way, the first- and second-order susceptibility is respectively defined as

$$\chi^{(1)}_{IJ}(\omega) = N\alpha_{IJ}(\omega)/[1 - (4\pi/3)N\alpha_{IJ}(\omega)] \quad (1)$$

and

$$\chi^{(2)}_{IJK}(\omega_3;\omega_1,\omega_2) = Nf_I(\omega_1)\, f_J(\omega_2)\, f_K(\omega_3)\, \beta_{IJK}(\omega_3;\omega_1,\omega_2) \quad (2)$$

where $\alpha_{IJ}(\omega) = \Sigma_{ij} C_{Ii} C_{Jj} A_{ij}(\omega)$ and $\beta_{IJK}(\omega_3;\omega_1,\omega_2) = \Sigma_{ijk} C_{Ii} C_{Jj} C_{Kk} B_{ijk}(\omega_3;\omega_1,\omega_2)$. The variables i,j,k span the molecular axes, and I,J,K refer to axes in the laboratory-fixed coordinate, N is the microspecies number density, and $f_I(\omega_1)$ is the local field factor at radiation frequency ω_1. It may be noted here that the local-field correction factor for $\chi^{(1)}$ in eq 1 can be given by the denominator term, namely $[1 - (4\pi/3)N\alpha_{IJ}(\omega)]$ from which the f_I terms of eq 2 can also be calculated.[16]

The microscopic polarizabilities, α_{IJ} and β_{IJK} in the laboratory-fixed coordinates are related to A_{ij} and B_{ijk} in the molecule-fixed coordinate system by the direction cosine C_{Ll}, respectively. The A_{ij} and B_{ijk} are elements of the microscopic first- and second-order polarizability tensor, respectively. The orientation of the molecule-fixed coordinate is chosen to be the same as that of laboratory-fixed coordinate in the present study. Accordingly, we are only concerned with calculations of α_{ij} and β_{ijk}, and hereafter letter I,J,K is replaced by i,j,k individually.

In this study, a semiempirical model Hamiltonian INDO and uncoupled treatments are chosen to compute molecular polarizabilities. The applied field is not therefore included in the molecular Hamiltonian, and the first- and second-order polarizabilities are computed using time-dependent perturbation theory. Calculations are carried out on the free molecule (independent of field) and response involves the coupling of excited states, and the electronic excited states created by the perturbing laser field are treated as an infinite sum over unperturbed particle-hole states. In the INDO calculations,[17,18] we only consider the valence orbitals of the constituent atoms of H−silsesquioxane. The valence orbitals are 1s for H, 2s, 2p for O and 3s, 3p for Si whose orbital exponents ζ along with the other parameters used in calculations are listed in ref 19.

The individual components of frequency-dependent first- and second-order polarizability are calculated by the sum-over-states (SOS) method derived from this perturbation theory.[9,10] The extensive expressions of α and β can be written as follows:

$$\alpha_{ij}(\omega_1) = 1/\vec{h}\Sigma_m \mu_{gm}{}^i \mu_{mg}{}^j [(\varpi_{mg} - \omega_1)^{-1} + (\varpi_{mg} + \omega_1)^{-1}] \quad (3)$$

$$\beta_{ijk}(\omega_3;\omega_1,\omega_2) = 1/\vec{h}^2 P_f \Sigma_{mn} \mu_{gn}{}^i \mu_{nm}{}^j \mu_{mg}{}^k [(\varpi_{ng} - \omega_3)(\varpi_{mg} - \omega_2)]^{-1} \quad (4)$$

where $\omega_3 = -\omega_1 - \omega_2$; $\varpi_{ng} = \omega_{ng} + \Delta/\vec{h}$, $\varpi_{mg} = \omega_{mg} + \Delta/\vec{h}$; and $\vec{h}\omega_{ng}$ or $\vec{h}\omega_{mg}$ is the transition energy from ground to excited state. Δ is referred to as a shift energy and consists of a shift of all the excites states by this value. This is equivalent to the scissors approximation introduced by Levine and Allan for the case of bulk semiconductors.[20] In the present calculations, we set shift energy to be zero due to unknown experimental gap values in H−silsesquioxanes. In eqs 3 and 4, μ's are the transition moment matrix elements which can be expressed as a sum of one-electron integrals.[21] In eq 4, the P_f is a full permutation operator by which the Cartesian indices are to be permuted along with the over input and output frequencies. Equations 3 and 4 are referred to as the extensive SOS in order to distinguish from the original sum-over-states method (SOS).

TABLE 1: Calculated Linear Optical Properties of Silsesquioxanes at 1064 nm[a]

molecule	building unit	N (10^{21}/cm^3)	α (Å^3)	$\chi^{(1)}$	n	ϵ
T_4 ($H_4Si_4O_6$)	$5^0 4^0 3^4$ (T_d)	5.139	6.663	0.040	1.226	1.502
T_6 ($H_6Si_6O_9$)	$5^0 4^3 3^2$ (D_{3h})	3.426	4.617	0.017	1.101	1.213
T_8 ($H_8Si_8O_{12}$)	$6^0 5^0 4^6$ (O_h)	2.569	4.391	0.012	1.072	1.149
	$5^2 4^2 3^2$ (C_{2v})		4.088	0.011	1.067	1.138
T_{10} ($H_{10}Si_{10}O_{15}$)	$6^0 5^2 4^5$ (D_{5h})	2.055	4.001	0.009	1.052	1.107
T_{12} ($H_{12}Si_{12}O_{18}$)	$6^0 5^4 4^4$ (D_{2d})	1.713	2.470	0.004	1.027	1.054
	$6^2 5^0 4^6$ (D_{6h})		3.454	0.006	1.038	1.076
T_{14} ($H_{14}Si_{14}O_{21}$)	$6^0 5^6 4^3$ (D_{3h})	1.468	2.913	0.004	1.027	1.055
	$6^1 5^4 4^4$ (C_{2v})		1.960	0.003	1.018	1.037
	$6^3 5^0 4^6$ (D_{3h})		2.292	0.003	1.021	1.043
T_{16} ($H_{16}Si_{16}O_{24}$)	$6^0 5^8 4^2$ (D_{4d})	1.285	1.730	0.002	1.014	1.028
	$6^1 5^6 4^3$ (C_{3v})		1.923	0.002	1.016	1.031
	$6^4 5^0 4^6$ (D_{2d})		1.133	0.001	1.009	1.018

[a] Here, N is molecular density, α is polarizabilty, $\chi^{(1)}$ is susceptibility, n is refractive index, and ϵ is dielectric constant.

The SOS perturbation theory expressions for the first- and second-order polarizability indicate that one requires dipole matrix elements between ground and excited states, excitation energies (for α), and excited-state dipole moments (for β). Since the electric field perturbation $F\mu$ is a one-electron operator, eq 4 implies that only singly excited states will mix with the ground state, if the ground state is taken as a single determinant. Furthermore, the molecular orbital coefficients are taken from diagonalization of the excited states at the monoexcited configuration level, and the energy denominator comes from the same diagonalization. The SOS expansion is, in general, infinite since the applied optical field mixes the molecular ground state with many excited states. For the calculation of β, we generally truncate the infinite SOS expansion to a finite one over about 170 states after apparent convergence of β has been reached. Note that this truncation leads to a formally valid criticism of the SOS methodology in the calculation of α due to its slow convergence in the summation over states. In the present study, the SOS method within the given CI space has yielded a well-converged value of β as shown in section 3.2.

Structural Configurations. For the INDO/CI calculations, the configurations of H−silsesquioxanes shown in Figures 1a and 1b are taken from our previous work based on the nonlocal density approximation to the density function theory.[8] The calculated structural parameters of several T cages were found to be in good agreement with the corresponding experimental values. Generally, the calculated Si−H bond length is about 147 pm. Both the Si−O bond length and the O−Si−O bond angle show a small variation as cage size increases with respective values of about 170 pm and 110°. On the other hand, The Si−O−Si bond angles range from 137° to 148°. The structural parameters the T_n cages with $n = 4$, 6, 8, 10, 12, 14, and 16 are taken from Tables 1 and 2 of the ref 8 where we have also described the molecular connectivity of various T cages in terms of 3-valent 3-connected convex polyhedra. The vertex of the polyhedra represent the Si−H group and the edges represent the Si−O−Si linkage. The n N-member ring is then represented by the notation of N^n. Note that the orientation of coordinate system in these calculations is the same as that in the previous work.[8]

TABLE 2: Calculated Components of the Second-Order Polarizabity (β) and Second-Order Susceptibility ($\chi^{(2)}$) at 1064 nm for Silsesquioxanes[a]

		xzx	*yzy*	*zxx*	*zyy*	*zzz*	*xyz*	*xzy*	*zxy*
T_4 (T_d)	β						−0.248	−0.248	−0.249
	$\chi^{(2)}$						−0.848	−0.848	−0.851
T_8 (C_{2v})	β	0.079	0.155	0.071	0.154	0.146			
	$\chi^{(2)}$	0.098	0.191	0.088	0.190	0.180			
T_{12} (D_{2d})	β						0.082	0.082	0.080
	$\chi^{(2)}$						0.062	0.062	0.060
T_{14} (C_{2v})	β	0.020	0.025	0.022	0.028	−0.073			
	$\chi^{(2)}$	0.013	0.016	0.014	0.018	−0.046			
T_{16}(C_{3v})	β	0.165		0.167		0.009			
	$\chi^{(2)}$	0.091		0.092		0.005			
T_{16} (D_{2d})	β						−0.006	−0.006	−0.008
	$\chi^{(2)}$						−0.003	−0.003	−0.005

[a] The unit of β is 10^{-30} esu^{-1} cm^5, and that of $\chi^{(2)}$ is pm/V.

3. Results and Discussion

3.1. Linear Optical Properties. The frequency-dependent linear refractive index can be represented by

$$n^2(\omega) = 1 + 4\pi\chi^{(1)}(\omega) \tag{5}$$

in which the linear susceptibility $\chi^{(1)}(\omega)$ is given by eqs 1 and 3. We note here that the molecular number density N in eq 1 is defined as the product of mass density and Avogadro's constant divided by the molar mass. In this study, we use the value of the mass density of 1.812 g cm^{-3} for susceptibility calculations. This value of the mass density is obtained for $H_{12}Si_{12}O_{18}$ in the X-ray diffraction study[22] and is not expected to change significantly for the T assemblies considered here.

Table 1 shows the calculated results for the polarizability α of the T cages, linear susceptibility $\chi^{(1)}$, average dynamic refractive index $\langle n\rangle$, and dielectric constant ϵ for the T assemblies. The average dynamic refractive index $\langle n\rangle$ is calculated from the average polarizability defined as $\langle\alpha\rangle = (\alpha_{ii} + \alpha_{jj} + \alpha_{kk})/3$. Assuming that the symmetry considered for isolated cages remains the same for the silsesquioxanes assemblies considered here, the frequency dependence of $\langle n\rangle$ for various conformers of silsesquioxanes are shown in Figure 2.

Accordingly, the dispersion of various H−silsesquioxanes has a similar shape, and $\langle n\rangle$ increases as the cage size decreases irrespective of the conformational symmetry. T_4 has the largest refractive index and T_{16} has the smallest one among the T_n family which we considered here. For example, $\langle n\rangle$ of the T_4 (T_d) and T_{16} (D_{2d}) are about 1.226 and 1.009 at 1064 nm respectively (Table 1). Within a given T cage, a small variation in $\langle n\rangle$ is predicted with different conformations. For instance, $\langle n\rangle$ for T_{16} in 5^84^2 (D_{4d}), 6^44^6 (D_{2d}) and $6^15^64^3$ (C_{3v}) configurations is predicted to be 1.014, 1.009, and 1.016 respectively at 1064 nm (Table 1). Although, the calculations predict the largest value of $\langle n\rangle$ for T_4 and T_6, these silsesquioxanes are not yet prepared and are found to be relatively unstable in our previous theoretical work.[8] Table 1 also lists the average molecular polarizabilities $\langle\alpha\rangle$ of the isolated T_n cages showing its variation with the cage size.

A comparison of the calculated $\langle n\rangle$ of the T cages with the measured one of silsesquioxane films shows the underestimation of $\langle n\rangle$ by the theoretical model employed here. Given that the H−silsesquioxane thin film has a refractive index of 1.378 at 1064 nm, the calculated results for the T assemblies show the underestimation of $\langle n\rangle$ by approximately 25%. This is due to the well-known fact of slow convergence of $\langle n\rangle$ in the SOS method. Despite taking the summation well over 280 states the convergence of $\langle n\rangle$ is not reached in the present study (Figure 3).

TABLE 3: Calculated Dipole Transition Moments of the Low-Lying Excited States of and T_4 (T_d), T_8 (C_{2v}), and T_{16} (D_{2d})

	dipole transition moments (debye)		
excited state	T_4 (T_d)	T_8 (C_{2v})	T_{16} (D_{2d})
first	0.8776	0.9138	0.1985
second	0.5540	0.2344	0.2017
third	0.7345	0.3063	0.2820

3.2. Nonlinear Optical Properties. Before attempting to compute the variation of the second-order susceptibility with frequency for the T_n assemblies, it is necessary to investigate its convergence behavior to determine whether the results obtained in the model employed here are reliable. In Figure 3 we show the variation of the calculated largest susceptibility tensor component ($\chi^{(2)}$) with the number of states considered in the SOS calculation at the wavelength of 1064 nm. Accordingly, $\chi^{(2)}$ obtained from the summation over 250 states is well-converged. Note that the local field correction factor (i.e., $f = (\epsilon + 2)/3)$) and molecular density number are assumed to be constant for the T_n assemblies and are taken from T_{12} to calculate $\chi^{(2)}$ in this work.

The components of dynamic second-order susceptibility calculated at 1064 nm for each T_n assembly (n = 4, 8, 12, 14 and 16) is given in Table 2. The largest susceptibility element is the $\chi_{xyz}(-2\omega;\omega,\omega)$ of −0.85 pm/V for T_4 with T_d symmetry and the second one is the $\chi_{yzy}(-2\omega;\omega,\omega)$ of 0.19 pm/V for T_8 with C_{2v} symmetry. Moreover, we can see from Figure 4 that the first peaks for T_8 and T_{16} are localized about 4 eV. The peaks in this frequency region are attributable to a two photon resonance. In this process, molecular assembly electron makes a transition from its ground state to an excited state by simultaneous absorption of two laser photons, for which the energy of each photon is larger than a half band gap energy. The energies of these peaks can therefore correspond to the calculated HOMO−LUMO gap energies of the T_n cages.[8] Overall, the calculated largest susceptibility elements show a decreasing tread from T_4 to T_{16} at below the frequency of 3.0 eV/h and have a very small dispersion with almost constant value at below 3 eV/h for each case.

In the context of the SOS method, the first- and second-order polarizabilities (given by eqs 3 and 4) are governed by the product of the transition dipole moments and the transition energy. For the T_n assemblies considered in this work, the transition energies (i.e., HOMO−LUMO gap) are expected to remain almost constant, as also shown in the previous work.[8] Hence, calculations of polarizabilities and hyperpolarizabilities for the T_n assemblies mostly depend on the dipole transition moments which, in fact, depend on the state function and spatial configuration. In Table 3, we list the dipole transition moments of the first three low-lying excited states for T_4, T_8, and T_{16} cages. Accordingly, the transition moments show a decreasing trend with the increase in the cage size, thereby suggesting a smaller susceptibility values for larger T_n assemblies, as also predicted here.

In the above discussion of the nonlinear susceptibility, we only concern with the second-harmonic generation (SHG), that is $\omega_1 = \omega_2$ in eqs 2 and 4. The linear electrooptic (LEO) susceptibility can also be computed if we set $\omega_2 = 0$ in eqs 2 and 4. Figure 4 also shows the calculated results for T_8 and T_{16}. As expected, the LEO values are predicted to be the same as those obtained from the SHG calculations at low-frequency

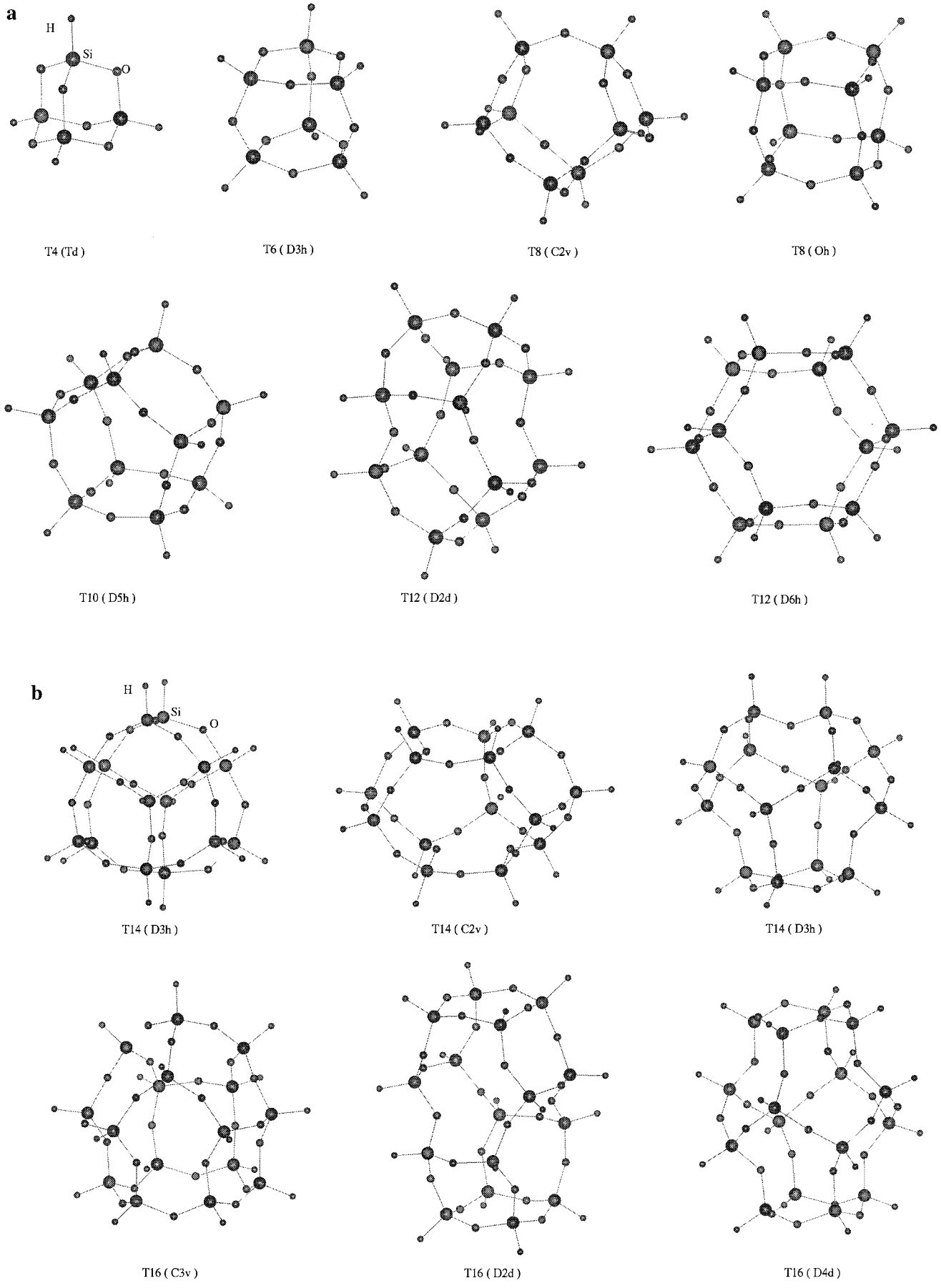

Figure 1. (a) Structural configurations of the T_4, T_6, T_8, T_{10}, and T_{12} cages taken from ref 8. (b) Structural configurations of the T_{14} and T_{16} cages taken from ref 8.

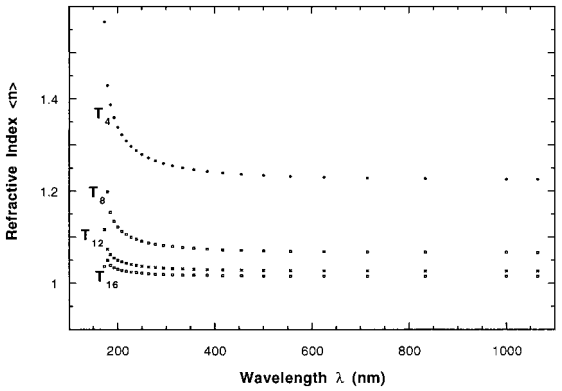

Figure 2. Variation of the average refractive index with wavelength for the T_n assemblies.

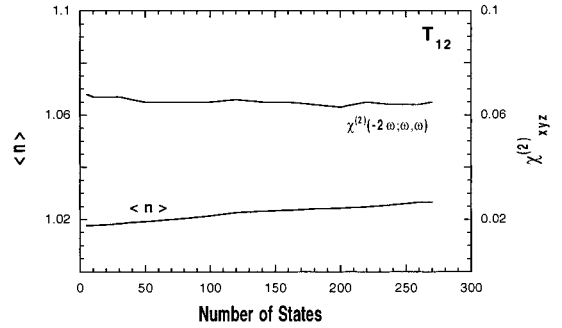

Figure 3. Convergence behavior of $\langle n \rangle$ and $\chi_{xyz}(-2\omega;\omega,\omega)$ with number of states considered in the SOS calculations for T_{12}.

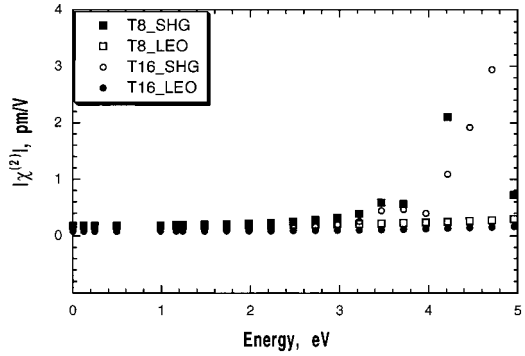

Figure 4. Frequency dependence of SHG ($\chi_{xyz}(-2\omega;\omega,\omega)$) and LEO ($\chi_{xyz}(-\omega;\omega,0)$) of T_8 and T_{16}.

region. In general, $\chi_{xyz}(-\omega;\omega,0)$ has a very small dispersion of the T_8 assemblies.

Next, we choose the T_8 assembly with *mm*2 crystal symmetry (point group symmetry C_{2v}) as an example to perform a comprehensive study of the second-order susceptibility. Note that this molecule is stable and is suggested to be a suitable staring molecule to synthesize the other silsesquioxanes. It is well-known that the second-order susceptibility tensor for mm2 symmetry have seven nonvanishing tensor elements which are reduced to five elements after considering the intrinsic permutation symmetry. Their frequency dependence for T_8 is shown in Figure 5. The calculated results confirm the validity of the Kleinman symmetry (i.e., $zxx = xzx$, and $zyy = yyz$ at below the frequency of 3.0 eV/h). For example, the calculated *xzx* and *zxx* is 0.10 and 0.09 pm/V, respectively, and both *zyy* and *yzy* are 0.19 pm/V at 1.165 eV/h. At above frequency of 3.0 eV/h, the $\chi^{(2)}$ dispersion curves show that the frequency doubling will be enhanced near resonance (Figure 5), and the Kleinman symmetry is invalid (i.e., $zxx \neq xzx$ and $zyy \neq yzy$).

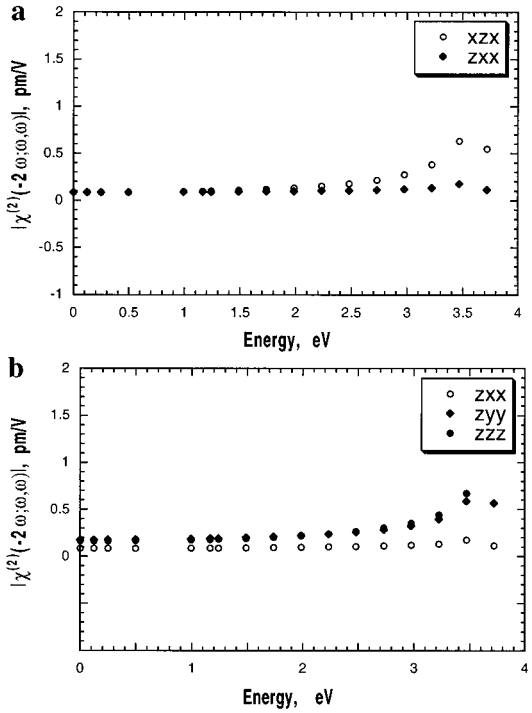

Figure 5. (a) Frequency dependence of $\chi_{xzx}(-2\omega;\omega,\omega)$ and $\chi_{zxx}(-2\omega;\omega,\omega)$ for T_8. (b) Frequency dependence of $\chi_{zxx}(-2\omega;\omega,\omega)$, $\chi_{zyy}(-2\omega;\omega,\omega)$, and $\chi_{zzz}(-2\omega;\omega,\omega)$ for T_8.

In the absence of experimental results for the second-order susceptibility for the *T* assemblies, we can only make comparison with the experimental value of d_{11} (i.e., $0.5\chi_{xxx}$) for crystalline α-quartz which is reported to be about 0.30 pm/V.[23] We find that the calculated $\chi^{(2)}$ for T_4 and T_8 assemblies (Table 2) is comparable in magnitude with that of α-quartz. However, we note here that calculations based on eq 4 (i.e., molecule superposition methodology) generally underestimate the local field correction factor $f = (\epsilon + 2)/3$, if the ϵ is taken from the SOS calculations.

Alternatively, a comparison between hyperpolarizabilities of T_8 and α-quartz can also be made. Using eq 4 and the experimental value of χ_{xxx}, β_{zzz} of α-quartz is found to be 0.017×10^{-30} esu^{-1} cm^5 which is much smaller than the calculated β_{zzz} of 0.15×10^{-30} esu^{-1} cm^5 for T_8 at 1064 nm.[24] On the basis of this comparatively large value of β_{zzz}, we therefore suggest that the T_8 cages can be introduced into the polymeric backbone to provide low optical loss while maintaining a high solubility of polymers for applications in the area of nonlinear optics.

4. Summary

In this work, we have employed the sum-over-states (SOS) method at the INDO/CI level to calculate polarizabilities and hyperpolarizabilities of H−silsesquioxanes, and then used the molecule superposition methodology to calculate their linear and nonlinear susceptibilities and the frequency dependence of $n(\omega)$ and $\chi^{(2)}(-2\omega;\omega,\omega)$. The calculated results show that the T_n assembly with a smaller cage has larger refractive index, dielectric function, SHG, and LEO susceptibilities. The SHG susceptibility of T_8 is predicted to be of the same order of magnitude as measured for crystalline α-quartz. Furthermore, both linear and nonlinear susceptibilities decrease with the increase in the cage size of the T_n assemblies. Finally, it is suggested that the small T_n cages will be good candidates for a nonlinear optical material in which the silsesquioxane-containing

part provides high transparency over a wide wavelength range, and adequate susceptibility in the ultraviolet or vacuum ultraviolet region of the optical spectrum.

Acknowledgment. This project was financially supported by the Dow Corning Corp. W.-D.C. acknowledges helpful conversations with Dr. J.-T Chen of Fujian Institute of Research on the Structure of Matter. K.X. acknowledges the Michigan Technological University for a Graduate Research Fellowship.

References and Notes

(1) Calzaferri, G. in Tailor-made silicon oxygen compounds: from molecules to materials, Corriu, R.; Jutzi, P., Eds.; Braunschweig: Wiesbaden, Germany, 1996.

(2) Bornhauser, P.; Calzaferri, G. *J. Phys. Chem.* **1996**, *100*, 2035.

(3) Hendan, B. J.; Marsmann, H. C. *J. Organomet. Chem.* **1994**, *483*, 33.

(4) Day, V. W.; Klemperer, W. K. *J. Am. Chem. Soc.* **1987**, *109*, 5554.

(5) Marcolli, C.; Calzaferri, G. *J. Phys. Chem. B* **1997**, *101*, 4925.

(6) Lee, S.; Makan, S.; Banazak Holl, M. M.; McFeely, F. R. *J. Am. Chem. Soc.* **1994**, *116*, 11819.

(7) Chandra, G. *Mater. Res. Soc. Symp. Proc.* **1991**, *203*, 97.

(8) Xiang, K.-H.; Pandey, R.; Pernis, U. C.; Freeman, C. *J. Phys. Chem. B* **1998**, *102*, 8704.

(9) Ward, J. F. *Rev. Mod. Phys.* **1965**, *37*, 1.

(10) Orr, B. J.; Ward, J. F. *Mol. Phys.* **1971**, *20*, 513.

(11) Bella, S. D.; Ratner, M. A.; Marks, T. J. *J. Am Chem. Soc.* **1992**, *114*, 5842.

(12) Cheng, W.-D.; Huang, J.-S.; Lu, J.-X. *Phys Rev. B* **1998**, *57*, 1527.

(13) Jiang, H.; Kakkar, A. K. *Macromolecules* **1998**, *31*, 4170. Jiang, H.; Kakkar, A. K. *Macromolecules* **1998**, *31*, 2501.

(14) Bremmer, J. N.; Liu, Y.; Gruszyuski, K. G.; Dall, F. C. *Mater. Res. Soc. Symp. Proc.* **1997**, *476*, 37.

(15) Fejer, M. M. *Physics Today Special Issue of Nonlinear Optics* **1994**, 25.

(16) Boyd, R. W. *Nonlinear optics*; Academic Press: New York, 1992.

(17) Bacon, A. D.; Zerner, M. C. *Theor. Chim. Acta* **1979**, *53*, 21.

(18) Anderson, W. P.; Cundari, T. R.; Zerner, M. C. *Int. J. Quantum Chem.* **1991**, *39*, 31.

(19) The input parameters are as follows. Slater exponents: H, $\zeta_{1s} = 1.20$ Å^{-1}; O, $\zeta_{2s,2p} = 2.275$ Å^{-1}; Si, $\zeta_{3s,3p} = 1.520$ Å^{-1}. Valence state ionization energies: H, $I_{1s} = -13.06$ eV; O, $I_{2s} = -32.49$ eV, $I_{2p} = -15.88$ eV; Si, $I_{3s} = -14.79$ eV, $I_{3p} = -8.10$ eV. Coulomb repulsion integrals: H, $\gamma = 12.85$ eV; O, $\gamma = 13.00$ eV; Si, $\gamma = 7.57$ eV. Resonance integrals: H, $\beta = -12.00$ eV; O, $\beta = -34.00$ eV; Si, $\beta = -9.00$ eV.

(20) Levine, Z. H.; Allan, D. C. *Phys. Rev. Lett.* **1989**, *63*, 1719.

(21) Pariser, R. J. *Chem. Phys.* **1956**, *24*, 250.

(22) Tönroos, K. W.; Burgi, H.-B.; Calzaferri, G.; Burgi, H. *Acta Crystallogr.* **1995**, *B51*, 155.

(23) Dmitriev, V. G.; Gurzadyan, G. G.; Nikogosyan, D. N. In *Handbook of Nonlinear Optical Crystals*, 2nd ed.; Siegman, A. E., Ed.; Springer: Berlin, 1995; p 283.

(24) We calculate the second-order molecular polarizability from the experimental value of d_{11} for α-quartz as follows: $\beta_{xxx} = 2d_{11}/(NF) = [2 \times 0.30$ (pm/V)/$(26.552 \times 3.1113)] \times 2.3872 \times 10^{-33}$ esu^{-1} cm^5 $= 0.017 \times 10^{-30}$ esu^{-1} cm^5 where the molecular density number N is obtained from the mass density and formula mass;[24] the local field factor is given by $F = [(n(\omega)^2 + 2)/3]^2[(n(2\omega)^2 + 2)/3]$ with $n(\omega) = 1.5382$ at wavelength of 1083 nm and $n(2\omega) = 1.5514$ at 534 nm.[24] The conversion unit from pm/V to esu^{-1} cm^5 is 2.3872×10^{-33}.